TPM Vol. 32, No. S6, 2025
ISSN: 1972-6325
https://www.tpmap.org/

Open Access

MONITORING OF CARBON MONOXIDE (CO) WITH SENTINEL-5P SATELLITE IMAGES FOR THE PROVINCE OF AREQUIPA

VERA ORTEGA DANNA JAMILA
MAGISTER SCIENTIAE IN WATER RESOURCES
STUDENT, ENGINEERING FACULTY, UNIVERSIDAD PRIVADA DEL NORTE, LIMA, PERÚ.
EMAIL: n00310119@upn.pe, ORCID ID: 10009-0009-4876-3035

PEREZ LAURA NOEMI GERALDINE
STUDENT, ENGINEERING FACULTY, UNIVERSIDAD PRIVADA DEL NORTE, LIMA, PERÚ.
EMAIL: n00243166@upn.pe, ORCID ID: 20009-0003-8519-0922

DIAZ TERRONES JOSE LUIS
STUDENT, ENGINEERING FACULTY, UNIVERSIDAD PRIVADA DEL NORTE, LIMA, PERÚ.
EMAIL: n00227685@upn.pe, ORCID ID: 30009-0003-5849-5712

CORNEJO MELENDEZ JHEREMY ALEXIS
STUDENT, ENGINEERING FACULTY, UNIVERSIDAD PRIVADA DEL NORTE, LIMA, PERÚ.
EMAIL: n00299936@upn.pe, ORCID ID: 40009-0001-0625-922X

TEJADA DIAZ FLAVIO JOSSEPITH
STUDENT, ENGINEERING FACULTY, UNIVERSIDAD PRIVADA DEL NORTE, LIMA, PERÚ.
EMAIL: n00298857@upn.pe, ORCID ID: 50009-0008-0004-427X

CARMONA ARTEAGA ABEL
RESEARCHER, ENGINEERING FACULTY, UNIVERSIDAD PRIVADA DEL NORTE, LIMA, PERÚ.
GRUPO DE INVESTIGACIÓN Y DESARROLLO E INNOVACIÓN UPN-IDIUPN
EMAIL: abel.carmona@upn.edu.pe, ORCID ID: 60000-0003-2895-9582

Abstract— In recent years, the Arequipa region has experienced a notable increase in air pollution caused by carbon monoxide (CO), primarily due to harmful human activities and forest fires. CO poses serious risks to both human health and the environment, as it is linked to respiratory and cardiovascular diseases, as well as strokes. Due to the limited availability of air quality monitoring stations in the area, this study utilized Sentinel-5P satellite imagery and the Google Earth Engine (GEE) platform to assess CO concentrations across the districts of the Arequipa province. The analysis covers the period from 2019 to 2023, offering valuable insights that can inform the development of effective air pollution mitigation strategies in the region.

Index Terms— Arequipa Region, Sentinel 5P, Google Earth Engine, GEE, Carbon Monoxide, CO.

INTRODUCTION

Air is fundamental to human survival, representing one of the most critical resources for life, yet it is often overlooked due to human activities. Among the primary pollutants we release is carbon monoxide (CO) [1]. CO is a common atmospheric pollutant, and its exposure poses significant health risks, being linked to respiratory diseases, cardiovascular conditions, and strokes [2]. Furthermore, air pollution caused by CO adversely impacts environmental quality, contributing to global warming and climate change [3].

Peru, like other developing nations, struggles with significant environmental pollution that has led to a decline in air quality[4]. One of the main contributors to this issue is the burning of agricultural waste, which emits various air pollutants such as carbon monoxide, nitrogen oxides, volatile organic compounds, and soot particles.

For many years, wildfires on Earth occurred naturally, but human intervention has significantly altered this dynamic. In Peru, nearly all wildfires are caused by human activities, primarily the use of fire to clear agricultural land and burn pastures. Despite existing restrictions, reports of wildfire emergencies have increased in recent years [6]. In Arequipa, poor agricultural practices, such as weed burning, have persisted despite established regulations,

continuing to drive wildfire incidents to this day [7]. This is illustrated in Figure 1.
Despite the importance of monitoring these pollutants, many rural areas in Peru, including regions within the province of Arequipa, lack adequate monitoring systems, limiting the effective management of atmospheric gas emissions [8]. In these areas, the use of monitoring networks such as Sentinel-5P provides an effective solution for obtaining accurate, real-time data on atmospheric pollutant concentrations, including carbon monoxide, enabling the efficient monitoring of large regions [9].

Fig. 1. Fires caused by poor agricultural practices [7].

In this context, the need for effective monitoring of CO concentrations within the district areas of the Arequipa province becomes evident, particularly considering the impact of agricultural practices on air quality.

OBJECTIVE

This study aims to monitor carbon monoxide (CO) levels across the districts of the Arequipa province by examining both their temporal and spatial patterns. To conduct this analysis, the research employed custom-built JavaScript algorithms within the Google Earth Engine (GEE) environment, allowing for the retrieval of CO data from the SENTINEL-5P satellite's gridded dataset.
The overarching goal is to evaluate the distribution and intensity of CO pollution in Arequipa between 2019 and 2023. Through this effort, the research intends to highlight trends in CO emissions and provide essential insights to support the formulation of air quality improvement strategies.

THEORETICAL FRAMEWORK

A. Carbon Monoxide (CO)
CO is a dangerous, colorless, and odorless gas, which makes its detection difficult without specialized equipment. It is produced from the incomplete combustion of organic compounds, such as fossil fuels, with its main sources including vehicle exhaust, smoke from fires, malfunctioning heating or cooking systems, and industrial processes like those in chemical plants or smelters [10].

Fig 2. Representation of CO gas [11].

Although atmospheric air typically does not contain CO, this gas can accumulate indoors or in poorly ventilated areas, posing a serious health risk. When inhaled, CO enters the bloodstream and interferes with oxygen transport, which can lead to symptoms ranging from headaches to death in severe cases. Prolonged exposure, even at low concentrations, can damage several body systems [12]. In addition to being a health hazard, CO also contributes to

environmental degradation [10].

B. Cartographic Information

For this study, the district boundaries and the geographical location of the district capitals in the Arequipa province, located in the Arequipa department, were used. The information was obtained from the national maps of the National Geographic Institute (IGN) at a 1:100,000 scale. The maps employed were as follows: 32s, 32t, 32u, 33r, 33s, 33t, 33u, 34r, 34s, 34t, and 34u.

C. Study Area

The study area is the Arequipa province, located in the Arequipa department. The population of each district is shown in Table I.

TABLE I Location of the capitals and the population by district in the Arequipa province

Nº	Districts	X	Y	Number of Inhabitants
1	Socabaya	-71.5288	-16.4674	78762
2	Jacobo Hunter	-71.5586	-16.4411	52426
3	Jose Luis Bustamante Y Rivero	-71.5238	-16.4277	84251
4	Tiabaya	-71.5914	-16.4497	17102
5	Sachaca	-71.5667	-16.4246	25612
6	La Joya	-71.8180	-16.4235	35943
7	Paucarpata	-71.5043	-16.4329	135923
8	Santa Rita De Siguas	-72.0938	-16.4940	6962
9	Arequipa	-71.5370	-16.3988	57847
10	Yanahuara	-71.5429	-16.3871	26512
11	Mariano Melgar	-71.5056	-16.4070	63899
12	Miraflores	-71.5223	-16.3942	62895
13	Chiguata	-71.3922	-16.4028	3128
14	Alto Selva Alegre	-71.5217	-16.3855	88056
15	Cerro Colorado	-71.5604	-16.3767	207114
16	Cayma	-71.5456	-16.3815	99968
17	Vitor	-71.9354	-16.4657	4198
18	Yura	-71.7060	-16.2468	36455
19	Uchumayo	-71.6727	-16.4252	15391
20	Characato	-71.4839	-16.4685	14047
21	Santa Isabel De Siguas	-72.1016	-16.3207	771
22	Pocsi	-71.3895	-16.5189	493

23	San Juan De Siguas	-72.1270	-16.3491	691
24	Polobaya	-71.3689	-16.5662	931
25	Yarabamba	-71.4752	-16.5472	1458
26	San Juan De Tarucani	-71.0605	-16.1837	1490
27	Quequeña	-71.4513	-16.5574	5043
28	Mollebaya	-71.4666	-16.4875	5208
29	Sabandia	-71.4946	-16.4567	4511

This province has a population of 1,137,087 inhabitants and 1,553 towns, according to the latest census by the National Institute of Statistics and Informatics (INEI) in 2017 [13].

D. ArcGIS

It is a Geographic Information System (GIS) software that allows for the management, analysis, and visualization of geographic data. It offers advanced tools for creating maps, performing spatial analysis, and managing geodatabases [14]. ArcGIS is used in various fields, such as cartography, public service planning, and scientific visualization [15]. In this research, we used this software for locating the towns and interpolating the CO distribution across the entire Arequipa province.

E. Air Pollution Data

To extract CO records, the twenty-nine district capitals of the Arequipa province listed in Table 1 were evaluated. The numbering of these capitals is shown in Figure 3.

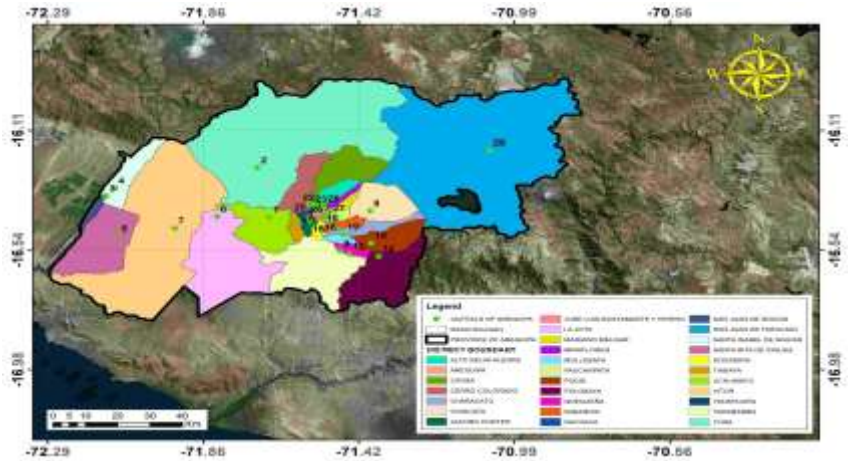

Fig. 3 Location of the capitals and district boundaries in the Arequipa province. Own elaboration.

F. Google Earth Engine (GEE)

It is a cloud computing platform launched by Google, designed for access to and processing of large-scale geospatial data [16]. GEE is essential for environmental monitoring and analysis as it processes geospatial data from satellites such as Sentinel and Landsat. It offers free services, benefiting developing countries. It is the most popular platform in Earth system science, used in fields such as agriculture, water management, and disaster assessment, and plays a key role in addressing current environmental challenges [17].

This information is collected through various satellites orbiting the Earth, from sources like the National Aeronautics and Space Administration (NASA) and the European Space Agency (ESA). Through this platform, records of accumulated CO measurements were obtained for the capitals and district areas of the province of Tacna [18].

It is important to note that GEE has a download limit of 5,000 records, so this must be taken into account when setting date ranges in the developed codes. Another aspect to consider is the noise in the data, where negative values are often detected in the vertical columns, especially in regions with low CO emissions or clean areas. It is recommended not to filter these values unless they are outliers, specifically vertical columns below -0.001 mol/m² [19].

G. Sentinel-5P

It is a polar satellite orbiting at an altitude of 817 km, crossing the equator at 13:30 LT with a 17-day repetition cycle. Its mission is to continue the data from previous missions such as SCIAMACHY and GOME-2, and pave the way for Sentinel-5. It provides daily global information on trace gases, aerosols, and clouds that affect air quality

and climate [20]. Its main instrument, TROPOMI, is a spectrometer that captures images in 8 bands, ranging from ultraviolet (UV) and visible to near-infrared (NIR) and shortwave infrared (SWIR), with a spatial resolution of 7×3.5 km, ideal for monitoring sources of pollutant emissions [21].
Sentinel-5P is the first Copernicus mission specifically designed to observe the atmosphere, monitoring air components such as ozone (O3), nitrogen dioxide (NO2), carbon monoxide (CO), sulfur dioxide (SO2), methane (CH4), formaldehyde (CH2O), aerosols, and clouds [22].
In Table II, the image collections used and the selected bands for calculating the contaminant measurement data, which were downloaded through the GEE platform, can be seen.

TABLE II Image collections used and selected bands for downloading data on pollutant measurements with GEE.

Image Collection (ID GEE)	**Selected Band**	**Description**	**Resolution (m)**
COPERNICUS/S5P/OFFL/L3_CO	CO_column_number_density	CO column density vertically integrated.	1113.2

Subsequently, a new variable was created with a function that generated the corresponding average image through code, based on a start and end date input by the user. Additionally, the geographic coordinates of the point from which the information needed to be extracted were inserted. Finally, the downloaded data was exported to a spreadsheet in Excel, with a geographic coordinate system (WGS84) and Geo TIFF format [23].

METHODOLOGY

This study used GEE as the sole information source due to the lack of local records for measuring pollutant gases in the study area. Upon downloading CO data, the annual quantities were summed, and the obtained values were compared at the coordinates of each district in the province of Arequipa. In this way, districts with the highest and lowest CO emissions were identified, and the results are presented below.
For the research, several scripts in JavaScript were developed to extract the variables of the analyzed pollutant gas. These codes are linked to raster images captured by the Sentinel-5P satellite.

H. Scripts for Extracting CO Data in District Capitals

In this research, a code was developed in JavaScript to download records from the gridded database of the Sentinel-5P satellite. For this purpose, a shapefile database was used, containing the locations of district, provincial, and departmental capitals in Peru, from which the ones presented in Table 1 were selected.
Below is the detailed code developed for this purpose.

Enter the study dates.

```
var startyear = 2019;
var endyear = 2023;
```

Create list of months to use in functions.

```
var months = ee.List.sequence(1,12);
```

Establish the beginning and end of the study.

```
var startdate = ee.Date.fromYMD(startyear,1,1);
var enddate = ee.Date.fromYMD(endyear,12,31);
```

Create list for variable years.

```
var years = ee.List.sequence(startyear,endyear);
```

The geometry must be loaded in shapefile format, which can represent a watershed or a specific area. In this case, the lines of the script load the shapefile of the district capitals of Peru and filter it according to the province of study.

```
var area_estudio = ee.FeatureCollection('projects/ee-dannavera/assets/capitales_Peru')
.filter(ee.Filter.eq('PROV','AREQUIPA'))
```

After this, the lines of code call the raster image collection corresponding to the gas being evaluated.

```
var P = ee.ImageCollection("COPERNICUS/S5P/OFFL/L3_CO")
.select('CO_column_number_density')
.filterDate(startdate, enddate)
//.sort('system:time_start', false)
.filterBounds(area_estudio);
```

Next, the part of the code is developed that will sum all the pixel concentrations at the specific location of each district capital listed in Table I.

```
var precipitacion_anual_acum = ee.ImageCollection.fromImages(
years.map(function (year) {
var annual = P.filter(ee.Filter.calendarRange(year, year, 'year'))
.sum()
.clip(area_estudio);
return annual
.set('year', year)
.set('system:time_start', ee.Date.fromYMD(year, 1, 1));
}));
```

Finally, a section was included in the code to calculate the daily accumulated concentration of the studied gas for each year, generating a graph that represents these data. Additionally, the option to download the results in CSV format was enabled for further analysis.

```
var chartP_anual = ui.Chart.image.seriesByRegion({
imageCollection: precipitacion_anual_acum,
regions: area_estudio,
reducer: ee.Reducer.sum(),
band: 'CO_column_number_density',
scale: 1100,
xProperty: 'system:time_start',
seriesProperty: 'DIST'})
.setOptions({
hAxis: {title: 'Intervalo de tiempo'},
title: 'Concentración acumulada anual de CO para cada area distrital',
vAxis: {title: ' Concentración (mol/m2)'}}
)
.setChartType('ColumnChart');
print(chartP_anual)
```

Similarly, lines of code were added to the script to replicate the calculation of the accumulated values on a monthly basis. The script, developed by Mg. Sc. Abel Carmona Arteaga for this purpose, is presented below [24].

I. Scripts to Extract CO Data in District Areas

This code will generate the annual and monthly cumulative sum of concentration across all district areas in the province under study. This script is similar to the one presented in section 4.1, with only a few minor modifications. In the following lines, the shapefile path was adjusted, and the field name for the province was changed to 'NOMBPROV' and for the districts to 'NOMBDIST'.

```
var area_estudio = ee.FeatureCollection('projects/ee-dannavera/assets/areas_distritales')
.filter(ee.Filter.eq('NOMBPROV','AREQUIPA'))
```

After this, we modified the part of the code:

```
var chartP_anual = ui.Chart.image.seriesByRegion({
imageCollection: precipitacao_anual_acum,
regions: area_estudio,
reducer: ee.Reducer.sum(),
band: 'CO_column_number_density',
scale: 1100,
```

```
xProperty: 'system:time_start',
seriesProperty: 'NOMBDIST'})
.setOptions({
hAxis: {title: 'Intervalo de tiempo'},
title: 'Concentración acumulada anual de CO para cada área distrital',
vAxis: {title: ' Concentración (mol/m2)'}})
.setChartType('ColumnChart');
print(chartP_anual)
```

The developed script is shown here [25].

J. Script for the Distribution of Accumulated CO

Although both scripts provide valuable information about the accumulated CO concentrations in the capitals and throughout the district areas, it is crucial to understand how CO is distributed across the entire Arequipa province.

Fig. 4 Shapefile of the districts in the provinces of Peru loaded. Own elaboration.

Therefore, a new code was developed to generate a raster file showing the accumulated CO distribution over a specific period. The development of this code is described below.

The first step involves uploading the four shapefiles corresponding to the district areas of the Arequipa province in the "Assets" section, as shown in Figure 4, and then proceeding with the "Upload" option.

Once the shapefile is uploaded

```
var param = {
P0:'2019-01-01',// FECHA INICIAL
P1:'2019-12-31'// FECHA FINAL
}
```

Subsequently, the lines of code call the raster image collection of the gas under study and apply a filter based on the previously entered dates.

```
var CO = ee.ImageCollection('COPERNICUS/S5P/OFFL/L3_CO').filterDate (param.P0,param.P1);
```

This section of the code calculates the total sum of the analyzed gas values for each pixel within the date range between P0 and P1, thereby displaying the gas distribution on the platform.

```
var SentinelCO = CO
.select('CO_column_number_density')
.filterBounds (geometry);
var COData = ee.Image(SentinelCO.sum());
var COClip = COData.clip (geometry);
Map.addLayer (COClip, {
max: 10,
min: 0,
palette: ["black", "blue", "purple", "cyan", "green", "yellow", "red"]},'Monoxido_de_Carbono-CO');
```

Finalmente, se exporta un archivo ráster en formato TIFF al Google Drive del usuario utilizando el siguiente código.

```
Export.image.toDrive({
```

```
image: COClip.select("CO_column_number_density"),
description: 'Monoxido_de_Carbono-CO',
scale: 1100,
region: geometry});
```

The code is shown here [26]. Below, the results obtained are presented.

RESULTS

K. Total CO Accumulation in District Capitals

Figure 5 shows the total annual CO concentration for the districts of the Arequipa province from 2019 to 2023.

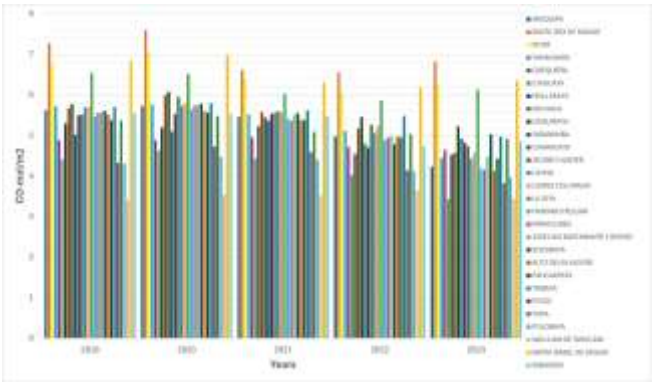

Fig. 5 Evolution of the annual CO concentration in the district capitals of the province of Arequipa between 2019, 2020, 2021, 2022, and 2023. Own elaboration.

Figure 6 illustrates the total monthly CO concentration for the years 2019, 2020, 2021, 2022, and 2023 for the capitals in the Arequipa province.

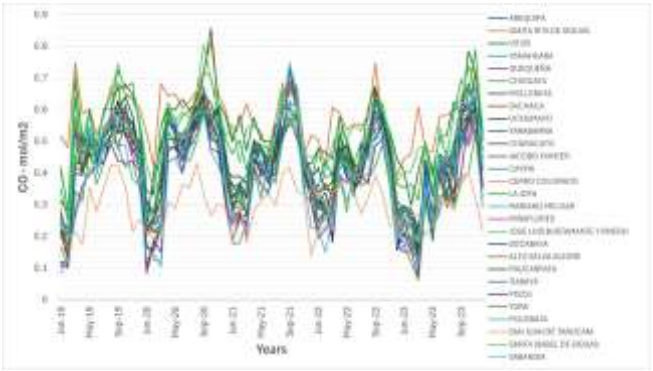

Fig. 6 Evolution of the monthly CO concentration in the district capitals of the province of Arequipa between 2019, 2020, 2021, 2022, and 2023. Own elaboration.

L. Total CO Accumulation in District Areas

According to Figure 7, the monthly CO concentration for district areas between 2019, 2020, 2021, 2022, and 2023 is as follows.

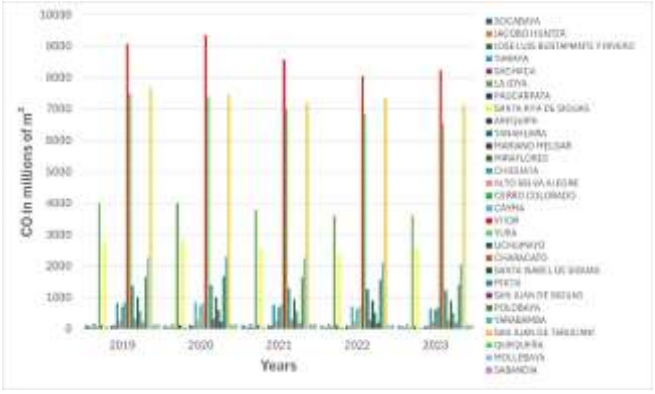

Fig. 7 Evolution of the monthly CO concentration in the districts of the province of Arequipa between 2019, 2020, 2021, 2022, and 2023. Own elaboration.

Figure 8 shows the total monthly CO concentration for the districts of the province of Arequipa between the years 2019, 2020, 2021, 2022, and 2023.

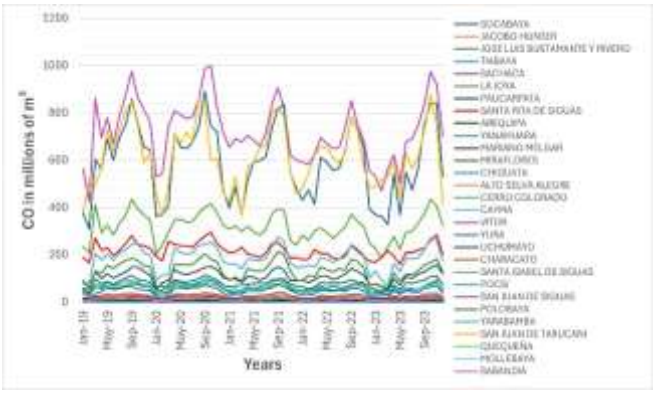

Fig. 8 Evolution of the monthly CO concentration in the districts of the province of Arequipa between 2019, 2020, 2021, 2022, and 2023. Own elaboration.

M. Annual Accumulated Spatial Representation of CO

Using the script developed in section 4.3 and uploaded into GEE, the annual CO distributions for the years 2019, 2020, 2021, 2022, and 2023 were obtained, as shown in Figure 9.

Fig. 9 Operation of the code created to represent the distribution of CO in the province of Arequipa. Own elaboration.

The raster information of CO concentration in mol/m² can be seen in Figures 10, 11, 12, 13, and 14.

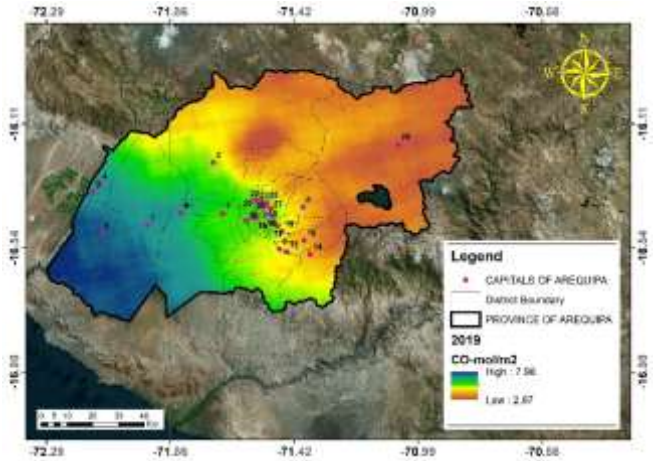

Fig. 10 Annual accumulated CO distribution in the Arequipa province during 2019. Own elaboration.

As shown in Figure 10, in 2019, the southwestern part of the province of Arequipa recorded maximum CO values of 7.98 mol/m². This can be attributed to forest fires that devastated hectares of vegetation cover across various districts in that year [27]. Meanwhile, in the central part of the province, average values of 5.47 mol/m² were

observed, and the northeastern district displayed the minimum values, which were around 2.97 mol/m².

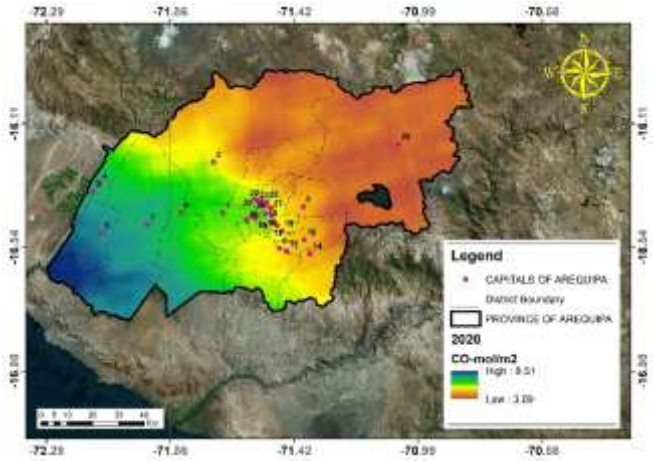

Fig. 11 Annual accumulated CO distribution in the Arequipa province during 2020. Own elaboration.

In 2020, CO concentrations ranged from minimum values of 3.09 mol/m², averages of 5.8 mol/m², to maximums of 8.51 mol/m². This year saw an increase in CO levels due to several fires caused by poor agricultural practices in the Arequipa region [28]. However, due to the challenges posed by the COVID-19 pandemic, the fires could not be controlled in a timely manner, resulting in significant increases in the concentration of this gas [29]. This is depicted in Figure 11.

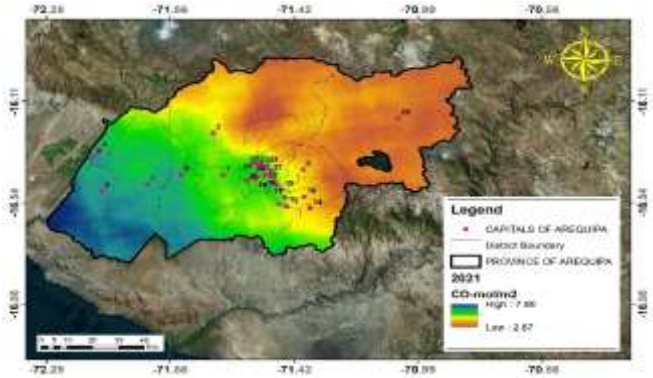

Fig. 12 Annual accumulated distribution of CO in the province of Arequipa during 2021. Own elaboration.

In 2021, SERFOR and regional governments joined efforts to improve the management of wildfire risks [30]. As a result of this initiative, a reduction in CO concentration was observed, with minimum values of 2.67 mol/m², averages of 5.28 mol/m², and maximum values of 7.9 mol/m². The highest concentrations were located in the southwest of the Arequipa province, particularly in the districts of Santa Rita and Vítor, as shown in Figure 12.
In 2022, based on initiatives such as workshops, training, and laws implemented by the Arequipa region to combat wildfires [31], a significant reduction in CO levels was observed compared to previous years. This year also saw an initiative to address the loss of wildlife, with over 4,000 trees being planted with the support of university students and SERFOR [32]. Consequently, CO concentrations ranged from minimum values of 2.61 mol/m², averages of 4.15 mol/m², to maximum values of 7.52 mol/m², as shown in Figure 13.

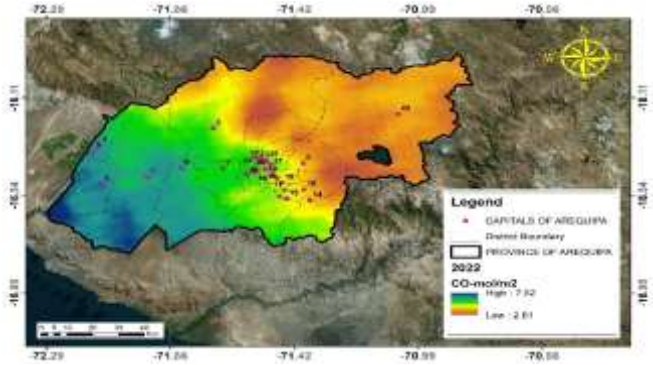

Fig. 13 Annual accumulated distribution of CO in the province of Arequipa during 2022. Own elaboration.

In Figure 14, values below 2.42 mol/m² and above 8.07 mol/m² are observed, indicating an increase in CO concentration in the higher areas of the district of Santa Rita de Siguas. This increase is believed to be related to a huaico in 2023 that affected irrigation channels and 15 hectares of crops, leading to the use of heavy machinery, causing intense rainfall, increasing soil erosion, and releasing particles into the air, thereby elevating CO levels in the district [33].

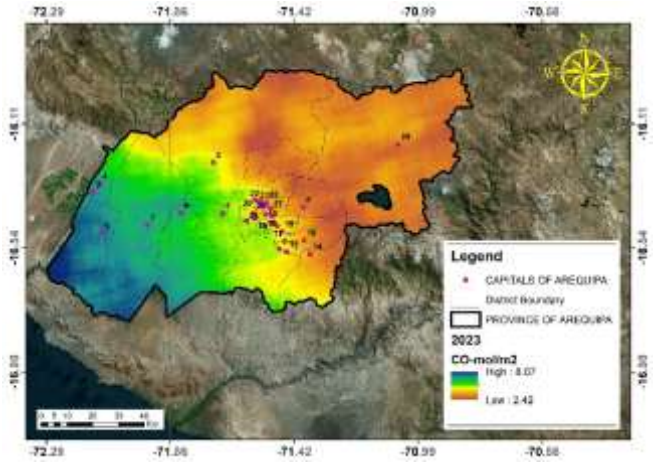

Fig. 14 Annual accumulated distribution of CO in the province of Arequipa during 2023. Own elaboration.

In Figure 15, we can observe the total accumulated CO in millions of m³ for each year across the entire area of the Arequipa province, which covers 8,117.09 km².

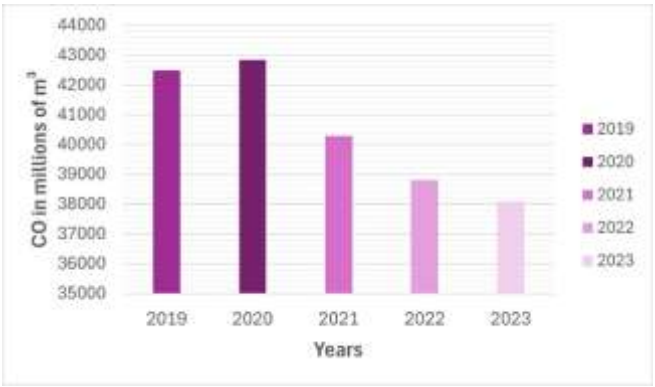

Fig. 15 Annual accumulation of CO in the province of Arequipa in millions of m³. Own elaboration.

CONCLUSIONS

This study indicates that CO emissions in the province of Arequipa peaked in 2020, coinciding with the pandemic period. Additionally, the district of Santa Rita de Sigua was identified as the district with the highest CO concentrations recorded over the last 5 years.

It can be observed that the CO concentrations during the 5-year study period are related to both low and high values depending on the intensity of agricultural activities, natural phenomena, and poor crop burning practices. Districts with less intensive activities exhibit lower CO concentrations.

In conclusion, the study on monitoring carbon monoxide in the province of Arequipa using satellite imagery can serve as a foundation for future research focused on reducing gas emissions.

REFERENCES

1. C. Chibueze, C. B. Afangideh y C. C. Nnaji (2023). «The menace and mitigation of air pollution in the built environment: A review,» Nigerian Journal of Technology, vol. 42, nº 1, pp. 12 – 29. Recuperado de https://www.ajol.info/index.php/njt/article/view/247191.

2. B. Li, J. Xiong, HX. Liu, D. Li y G. Chen (2022). «Devil or angel: two roles of carbon monoxide in stroke,» Medical Gas Research, vol. 12, nº 4, pp. 125-130. Recuperado de https://journals.lww.com/mgar/fulltext/2022/12040/Devil_or_angel__two_roles_of_carbon_monoxide_in.2.aspx

3. L. Manisalidis, E. Stavropoulou, A. Stavropoulos y E. Bezirtzoglou (2020). «Environmental and Health Impacts of Air Pollution: A Review,» Frontiers in Public Health, vol. 8. Recuperado de https://www.frontiersin.org/journals/public-health/articles/10.3389/fpubh.2020.00014/full
4. P. Córdova, T. O. Barrios y C. Córdova (2021). «Primera caracterización de emisiones contaminantes y la calidad del aire en Ica, Perú,» Rev Cub Quim, vol. 33, nº 1. Recuperado de http://scielo.sld.cu/scielo.php?pid=S2224-54212021000100138&script=sci_arttext
5. D-Y. Kim, M-A. Choi, Y-H. Han y S-K. Park (2016). «A Study on Estimation of Air Pollutants Emission from Agricultural Waste Burning,» Journal of Korean Society for Atmospheric Environmen, vol. 32, nº 2, pp. 167-175. Recuperado de https://jekosae.or.kr/_common/do.php?a=full&b=41&bidx=517&aidx=6458
6. S. Alvarez, R. Zubieta, A. M. Martínez y Y. C. Ccanchi (2023). «Uso del fuego y el rol de la población durante quemas e incendios forestales en Cusco» Boletín científico El Niño , Instituto Geofísico del Perú, vol. 10, nº 5, pp. 4-10. Recuperado de https://repositorio.igp.gob.pe/items/94ba4411-420a-49de-acda-fe91f67afadc
7. CORREO, 2020. Recuperado de https://diariocorreo.pe/edicion/arequipa/incendios-en-arequipa-se-originan-por-mala-practica-de-los-agricultores-947149/?ref=dcr
8. T. Holloway, D. Miller, S. Anenberg, M. Diao, B. Duncan, A. M. Fiore, D. K. Henze, J. Hess, P. L. Kinney, Y. Liu, J. L. Neu, S. M. O'Neill, M. Odman, R. Pierce, A. G. Russell, D. Tong, J. West y M. A. Zondlo (2021). «Satellite Monitoring for Air Quality and Health,» Annual Review of Biomedical Data Science, vol. 4, nº 1, pp. 417-447. Recuperado de https://www.annualreviews.org/content/journals/10.1146/annurev-biodatasci-110920-093120
9. D. Mejía, H. Alvarez, R. Zalakeviciute, D. Macancela, C. Sanchez y S. Bonilla (2023). «Sentinel satellite data monitoring of air pollutants with interpolation methods in Guayaquil, Ecuador,» Remote Sensing Applications: Society and Environment, vol. 31. Recuperado de https://www.sciencedirect.com/science/article/pii/S2352938523000721?via%3Dihub
10. H. Kinoshita, . H. Türkan, S. Vucinic, S. Naqvi, R. Bedair, R. Rezaee y . A. Tsatsakis (2020) «Carbon monoxide poisoning,» Toxicology Reports, vol. 7, pp. 169-173. Recuperado de https://www.sciencedirect.com/science/article/pii/S2214750019305864
11. Modelo vectorial de bola y palo de sustancia química: icono de la molécula", iStock, 2023. recuperado de: https://www.istockphoto.com/es/vector/modelo-vectorial-de-bola-y-palo-de-sustancia-qu%C3%ADmica-icono-de-la-mol%C3%A9cula-de-gm1281141046-379265072
12. J. Wiater y K. Gładyszewska-Fiedoruk (2022). «Idoor Air Quality with Particular Reference to Carbon Monoxide,» Journal of Ecological Engineering, vol. 23, nº 6, pp. 286-293. Recuperado de https://www.jeeng.net/Indoor-Air-Quality-with-Particular-Reference-to-Carbon-Monoxide-in-the-Room-A-Pilot,149284,0,2.html
13. INEI (2017). «Resultados Definitivos de los Censos Nacionales 2017» Censo 2017. Recuperado de https://censo2017.inei.gob.pe/resultados-definitivos-de-los-censos-nacionales-2017/
14. R. Hussein, H. Mahdi y H. Al-Shukri (2023). «Integrating GPR with ArcGIS Pro to map the Central Arkansas Water pipelines beneath the old Broadway Bridge, Little Rock,» Journal of Applied Geophysics, vol. 215. Recuperado de https://www.sciencedirect.com/science/article/pii/S0926985123002197
15. S. Phantuwongraj, P. Chenrai y T. Assawincharoenkij (2021). «Pilot Study Using ArcGIS Online to Enhance Students' Learning Experience in Fieldwork,» Geosciences, vol. 11, nº 9. Recuperado de https://www.mdpi.com/2076-3263/11/9/357
A.Velastegui, N. Montalván, P. Carrión, H. Rivera, . L. Sadeck y . M. Adami (2023). «Google Earth Engine: A Global Analysis and Future Trends,» Remote Sensing, vol. 15, nº 14. Recuperado de https://www.mdpi.com/2072-4292/15/14/3675
16. Q. Zhao, L. Yu, X. Li, D. Peng, Y. Zhang y P. Gong (2021). «Progress and Trends in the Application of Google Earth and,» Remote Sensing, vol. 13, nº 18. Recuperado de https://www.mdpi.com/2072-4292/13/18/3778
17. H. J. Manchay Tocto , H. V. Cobos Cauper , A. Carmona Arteaga y J. L. Neyra Torres (2023). «Nitrogen dioxide (NO2) monitoring with sentinel-5P satellite images for the province of Coronel Portillo,» Latin American and Caribbean Consortium of Engineering Institutions. Recuperado de http://dx.doi.org/10.18687/laccei2023.1.1.349
18. C. A. Pacheco Chávez, J. M. Vilchez Valverde, A. Carmona Arteaga y J. L. Neyra Torres (2023). «Monitoring of carbon monoxide (CO) with sentinel-5P satellite images for the province of Huanuco,» Latin American and Caribbean Consortium of Engineering Institutions. Recuperado de http://dx.doi.org/10.18687/laccei2023.1.1.400

N. Vîrghileanu, I. Săvulescu, B.-A. Mihai, . C. Nistor y R. Dobre (2021). «Nitrogen Dioxide (NO2) Pollution Monitoring with Sentinel-5P Satellite Imagery over Europe during the Coronavirus Pandemic Outbreak,» Remote Sensing, vol. 12, nº 21. Recuperado de https://www.mdpi.com/2072-4292/12/21/3575

19. Z. Zheng, Z. Yang, Z. Wu y F. Marinello (2019). «Spatial Variation of NO2 and Its Impact Factors in China: An Application of Sentinel-5P Products,» Remote Sensing, vol. 11, nº 16. Recuperado de https://www.mdpi.com/2072-4292/11/16/1939

A.Carbone, R. Restaino, G. Vivone y J. Chanussot (2024). «Model-Based Super-Resolution for Sentinel-5P Data,» IEEE Transactions on Geoscience and Remote Sensing, vol. 62, pp. 1-16. Recuperado de https://ieeexplore.ieee.org/document/10499875

A.G. Ochante Sanchez, H. . J. Manchay Tocto, A. Carmona Arteaga y N. Campos Vasquez (2023). «Monitoring of carbon monoxide (CO) pollution using Sentinel - 5P satellite images since the beginning of the Coronavirus pandemic (case study: Huamanga Province),» Latin American and Caribbean Consortium of Engineering Institutions. Recuperado de http://dx.doi.org/10.18687/laccei2023.1.1.368

20. Abel Carmona Arteaga (2023). Código en Google Earth Engine Extracción de CO para capitales distritales. Recuperado de https://code.earthengine.google.com/c2d05d451c6e581bf76163b21ff4543b
21. Abel Carmona Arteaga (2023). Código en Google Earth Engine Extracción de CO para áreas distritales. Recuperado de https://code.earthengine.google.com/dd389739a78950ecf046b8339c52323a
22. Abel Carmona Arteaga (2023). Código en Google Earth Engine Raster de gases contaminantes. Recuperado de https://code.earthengine.google.com/951deabf36e2226aa37a5fadb88b3a4d
23. Servicio Nacional Forestal y de Fauna Silvestre (Serfor), “Incendio forestal arrasó con más de 150 hectáreas en Arequipa”, 2019. Recuperado de:
24. https: //www.gob.pe /institucion /serfor /noticias /214523 -incendio-forestal -arraso-con -mas -de -150 -hectáreas -en-Arequipa.
25. Servicio Nacional Forestal y de Fauna Silvestre (Serfor), “Arequipa registró seis incendios forestales el último fin de semana”, 23-sep-2020.
26. Recuperado de: https ://www.gob .pe /institucion/serfor /noticias/303843 -arequipa -registro -seis -incendios--para-el -último-fin- de -semana
27. Servicio Nacional Forestal y de Fauna Silvestre (Serfor), “Los incendios forestales afectan la salud y hacen más vulnerables a las personas a contraer enfermedades”, 19-ago-2020.
28. Recuperado de: https : //www.gob.pe/en/ser para /noticias /29-los -incendios-para-afectan -la -s-y -hacen -mas -vulnerabilidad-a--las -personas -a -con-enfermedades.
29. Servicio Nacional Forestal y de Fauna Silvestre (Serfor), “Serfor y 18 gobiernos regionales articulan esfuerzo para optimizar la gestión de riesgos ante incendios forestales”, 11-jul-2021
30. Recuperado de: https://www.gob.pe/institucion/serfor/noticias/505404-serfor-y-18-gobiernos-regionales-articulan-esfuerzo-para-optimizar-la-gestion-de-riesgos-ante-incendios-forestales.
31. Servicio Nacional Forestal y de Fauna Silvestre (Serfor), “Arequipa: Serfor capacitó a más de un centenar de serenos en gestión de riesgos de desastres”, 17-oct-2022. Recuperado de:
https://www.gob.pe/institucion/serfor/noticias/672123-arequipa-serfor-capacito-a-mas-de-un-centenar-de-serenos-en-gestion-de-riesgos-de-desastres
32. Servicio Nacional Forestal y de Fauna Silvestre (Serfor), “Arequipa: estudiantes universitarios y pobladores siembran más de 4 mil árboles”, 22-nov-2022. Recuperado de:
https://www.gob.pe/institucion/serfor/noticias/673188-arequipa-estudiantes-universitarios-y-pobladores-siembran-mas-de-4-mil-arboles.
33. Autoridad Nacional del Agua (ANA), “Se inspección de daños en canales Santa Rita-Siguas”, 6 de abril de 2015. Recuperado de: https://www.iagua.es/noticias/peru/ana-peru/15/04/06/se-inspecciona-danos-canales-santa-rita-siguas